

How coupled elementary units determine the dynamics of macroscopic glass-forming systems

Christian Rehwald¹ and Andreas Heuer¹

¹*Institut für Physikalische Chemie, Westfälische Wilhelms-Universität Münster,
Corrensstrasse 28/30, 48149 Münster, Germany*

(Dated: October 30, 2018)

Abstract

We investigate the dynamics of a binary mixture Lennard-Jones system of different system sizes with respect to the importance of the properties of the underlying potential energy landscape (PEL). We show that the dynamics of small systems can be very well described within the continuous time random walk formalism, which is determined solely by PEL parameters. Finite size analysis shows that the diffusivity of large and small systems are very similar. This suggests that the PEL parameters of the small system also determine the local dynamics in large systems. The structural relaxation time, however, displays significant finite size effects. Furthermore, using a non-equilibrium configuration of a large system, we find that causal connections exist between close-by regions of the system. These findings can be described by the coupled landscape model for which a macroscopic system is described by a superposition of elementary systems each described by its PEL. A minimum coupling is introduced which accounts for the finite size behavior. The coupling strength, as the single adjustable parameter, becomes smaller closer to the glass transition.

I. INTRODUCTION

Understanding the complex dynamics of glassy materials such as supercooled liquids is still a highly controversial problem. In contrast to regular liquids the single particle dynamics in the supercooled state become spatially and temporally correlated, which leads to pronounced dynamical heterogeneities. Dynamical heterogeneities are a universal property of glass-forming systems and are responsible for several phenomena like non-exponential decay of response functions and the violation of the Stokes-Einstein relation.

In small model systems Vogel and coworkers [1] could show that particle rearrangements are typically localized and that their number does not depend on temperature. These findings could also be validated for large systems by Keys *et al.* [2]. The authors additionally related the propagation of motion to dynamical subunits which occur in a facilitation-like manner, meaning that excitations on one scale facilitate dynamics of neighboring excitations thereby creating excitations on larger scales. The characterization of facilitated dynamics in molecular dynamics (MD) simulations was attempted by different authors. For example Candelier and coworkers [3, 4] proved the aggregation of cage-breaking processes into avalanches in a granular system. Presently discussed models range between the old idea of Adam and Gibbs [5] of a qualitative decomposition of a sample into elementary subsystems and the facilitation approach, where all complexity emerges by more or less complex coupling rules. For example the kinetically constrained spin models were studied extensively by different authors [6, 7]. Dynamical facilitation can alternatively be formulated as a coupling process. Rehwald *et al.* [8] discovered from studying finite size effects, that these coupling processes determine structural relaxation properties. In shear experiments it was demonstrated that the range of coupling interactions, manifested by correlated particle displacements due to stress, covers just some particle diameters [9, 10]. Other groups report of long ranged elastic interactions in glycerol measured by dielectric relaxation [11].

A different approach, relating the dramatic slowing down of the dynamics at the glass transition to the potential energy landscape (PEL), was introduced by Goldstein [12]. He stated that at sufficiently low temperatures the system resides near local minima, so called inherent structures (IS), of the potential. While many computer simulations confirmed that the thermodynamics are indeed determined by the distribution of ISs, the connection with the dynamics could be revealed much later. For small systems it was possible to predict

the dynamics from parameters of the underlying potential energy landscape (PEL) [13–16] with the concept of metabasins. The dynamics between metabasins are closely related to the trap model [17, 18]. Many features of the complex glassy dynamics could be derived from PEL properties.

The situation changes when studying large systems: the PEL is no longer suitable for the prediction of the dynamics. Here we show that the PEL formalism can be extended to large systems by decomposing the system into elementary subsystems each of which is described by its own PEL. In contrast to kinetically constrained spin models the elementary subunits in this approach are complex systems, already reflecting macroscopic properties for thermodynamic observables [19] or self diffusion properties. Since thermodynamic properties do not change significantly when enlarging the system above a certain minimum size [19], and rearrangements are localized within a temperature independent size, we can be sure to capture the important relaxation properties in a single elementary subsystem. Additional fluctuations and interactions can then be included into the coupling rules between the subsystems. In terms of the complex nature of the elementary subsystem our approach resembles the mosaic approach [20] where the sample is decomposed into a mosaic of aperiodic crystals, so called entropic droplets. Nevertheless, in the mosaic approach all coupling processes are captured by the distribution of free energy barrier heights.

This manuscript is organized as follows: First we show how the minimum system can be described by the PEL and the continuous time random walk approach (CTRW), both analytically and numerically. After discussing changes of the CTRW when approaching larger system sizes we give a short summary of the physical scenario and motivate the presence of coupling effects. After discussing some technical questions concerning the used variables for the comparison between model and MD, we explicitly identify the presence of coupling processes via appropriate simulations. These findings motivate the coupled landscape model (CLM) which will be presented in the last section. It is shown that to a very good approximation the finite size effects of dynamic observables are fully captured by the CLM. Finally we figure out in how far the CLM is connected to recently discussed models.

σ	λ	e_c	κ	Γ_0	e_{cut}	σ_γ
2.9	0.50	-11.9	0.56	4.82	-25	1.0

TABLE I. Thermodynamic and dynamic PEL parameters for the binary mixture Lennard-Jones system with $N = 65$ and $e_0 = 0$.

II. THE MINIMUM SYSTEM

Throughout this paper we compare the model results with the binary mixture Kob-Andersen Lennard-Jones (BMLJ) system [21] applying periodic boundary conditions. Due to the small system size we have used a slightly shorter cutoff of $r_c = 1.8$ [14]. All MD simulations have been performed in the NVT ensemble using a Nosé-Hoover thermostat.

The PEL of a binary mixture of Lennard-Jones particles applying different system sizes was studied extensively [22]. One key result of Doliwa and Heuer [19] is the connection between states of the PEL, so called metabasins (MB), and the dynamics of the system. An MB can be constructed from a given trajectory of inherent structures by removing the complete forward-backward correlations between them. If the system is small enough, the mean waiting time $\langle\tau(e)\rangle$, during which the system resides in a MB, strongly depends on the energy e of the specific MB. Of course, the system cannot be too small because otherwise massive finite size effects set in regarding the thermodynamics [14]. In the same work it has been shown, that a system size of $N_{\min} = 65$ (BMLJ65) particles is a good choice for a minimum system. This minimum length scale of approx. 65 particles does not display any significant temperature dependence.

In the next step one has to determine how the specific properties of the potential energy landscape determine the dynamic properties of the liquid. Many properties will resemble the simple trapmodel [17, 23]. Here we summarize the most important results. The corresponding parameters, determined from appropriate simulations [22] are listed in Tab. I. Due to improved simulation data they slightly differ from those given in [22].

The shape of the density of states (DOS) $G(e)$ turned out to be close to a Gaussian $G(e) \sim \exp[-(e - e_0)/2\sigma^2]$ with an additional cutoff below e_{cut} . For low e the $G(e)$ decays slightly faster than expected from a Gaussian. For reasons of simplicity this is modeled by a cutoff energy e_{cut} and an additional factor $\exp[-(e - e_{cut})^\mu]$. For analytical results this factor will be neglected. In the trap model the escape out of a MB of energy e can be described by

a simple rate process with rate $\Gamma(e)$, given by $\Gamma(e) = \Gamma_0 \exp[\beta e]$. For the BMLJ65 system a slightly more complex energy dependence is observed [22]:

$$\frac{\Gamma(e)}{\Gamma_0} = e^{-\beta V_0} \begin{cases} \exp[\lambda(\beta + \kappa k_{\text{entro}})(e - e_c)] & , e < e_c \\ 1 & , e > e_c \end{cases}, \quad (1)$$

where Γ_0 defines the overall time scale. The escape from a MB of energy e is a multi-step process. The energy of the first IS after having completed the escape process is denoted by e_c . Due to percolation arguments e_c is independent of e [22]. The energy at the final barrier is given by $V_0 + e_c$, i.e. V_0 denotes the height of the last barrier crossed. The relaxation is solid-like (activated) for $e < e_c$, whereas it is liquid-like otherwise [24]. For $e < e_c$ an additional entropic term, involving the factor κk_{entro} , has to be taken into account, where $k_{\text{entro}} = (e_0 - e_c)/\sigma^2$. It reflects that the number of escape paths from a MB increases exponentially with decreasing MB energy. The limit $\kappa = 1$ can be rationalized in a simple PEL model [25]. For reasons of simplicity we chose the energy scale such that $e_0 = 0$ from now on. In the general case $\kappa < 1$ plays the role of an empirical factor of the order of one. If the investigated system contains M independent subsystems one gets $\lambda = 1/M$. Some additional implications of the choice $\lambda < 1$ will be discussed in the appendix.

As reported in [26], the width of the waiting time distribution at fixed energy e , expressed via $S(e) = \langle \tau^2(e) \rangle / \langle \tau(e) \rangle^2 - 1$, show deviations from an exponential distribution which disagrees with a pure rate process. This is, however, expected if the total system is a superposition of subsystems [22]. This broadening results from the fact that the total energy e can be decomposed in different ways. Formally, this broadening can be expressed by a distribution $\varpi(\gamma, e)$ of jump rates γ at fixed energy e . Here we approximate the γ -dependence of $\varpi(\gamma, e)$ by a log-normal distribution with variance σ_γ and mean value $\mu(e)$. Instead of an exponential distribution one gets $\omega(\tau, e) = \int d\gamma \varpi(\gamma, e) \gamma \exp[-\gamma\tau]$ as waiting time distribution for states of energy e . The moments of this distribution are related to the moments of γ via

$$\langle \tau^n(e) \rangle_\omega = n! \frac{\exp[n^2 \sigma_\gamma^2]}{\langle \gamma^n(e) \rangle_\varpi}. \quad (2)$$

In the MD simulation only $\langle \tau^n(e) \rangle$ can be calculated. Therefore one can estimate σ_γ by the relation

$$\sigma_\gamma^2 = \ln \left[\frac{\langle \tau^2(e) \rangle_\omega}{2 \langle \tau(e) \rangle_\omega^2} \right] \quad (3)$$

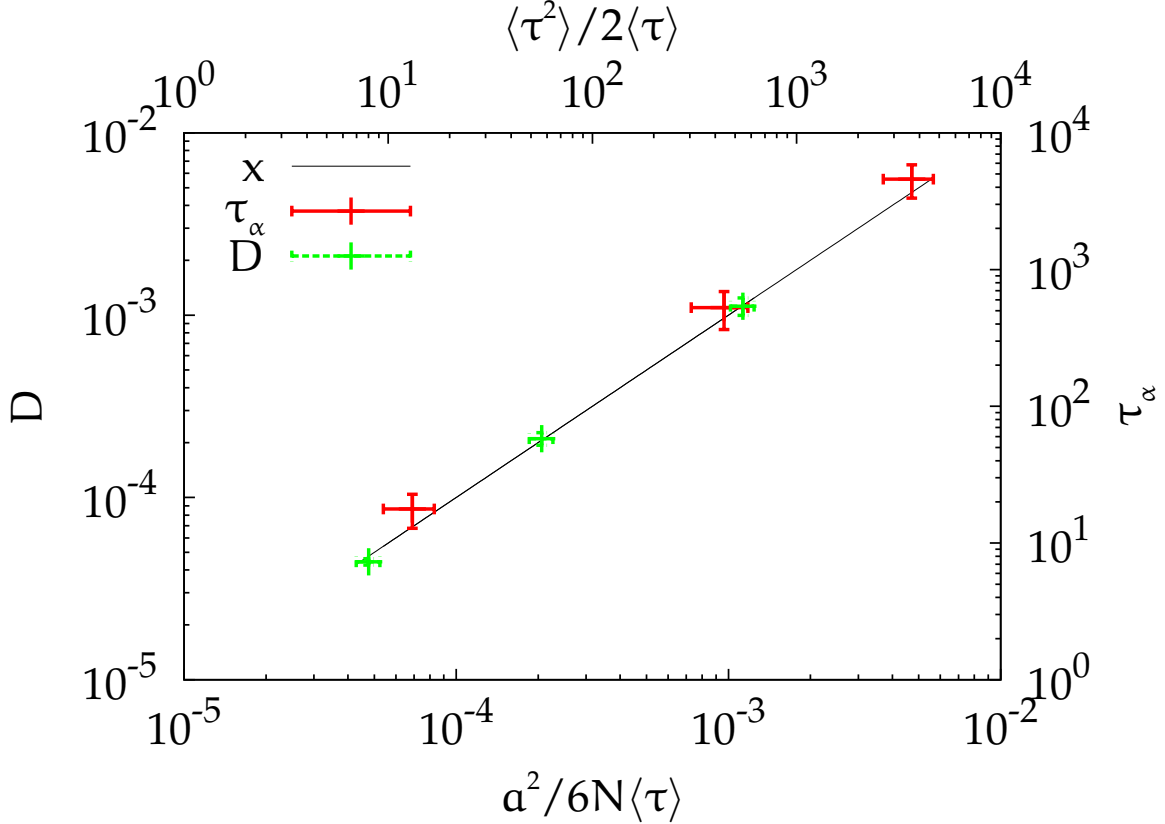


FIG. 1. Comparison of the absolute values of D and τ_α from the MB trajectory with corresponding expressions from the CTRW PEL description. Included is the diagonal.

We calculate the right hand side of equation (3) from MB trajectories and find that σ_γ is approx. 1.0, corresponding to a broadening of one order of magnitude. It is slightly temperature dependent and can to a good approximation be assumed to be constant in the relevant energy range. The distribution $\varpi(\gamma, e)$ is very narrow compared to the equilibrium distribution of rates $p(\log \Gamma)$ (standard deviation at $T = 0.5$ is approx. 4.4). We note in passing, that for $\sigma_\Gamma > 0$ the energy of a state is no longer solely sufficient to describe the specific rate γ of a MB.

As shown in [27] the dynamics can be described as a CTRW in configuration space. Therefore the most relevant transport coefficients like D or τ_α can be calculated analytically by solving the Gaussian integrals $\int \Gamma^n(e) p_{eq}(e) de$ [28]. Beyond the high temperature limit (no influence of the crossover energy) results for $\lambda = \kappa = 1$ can be found in literature like the well-known quadratic behavior $\tau_\alpha \propto \exp[\sigma^2(\beta - \beta_0)^2]$ with $\beta_0 = -k_{\text{entro}}$ [2, 22, 29]. For

general $\lambda < 1$ the T -dependence of D and τ_α is not purely quadratic (see Appendix A). However, for the Stokes-Einstein relation one again obtains a quadratic dependence

$$\ln [D\tau_\alpha] \sim \ln [\langle \Gamma^{-1} \rangle \langle \Gamma \rangle] = \lambda^2 \sigma^2 (\beta + \kappa k_{\text{entro}})^2. \quad (4)$$

In the low temperature limit one gets $D\tau_\alpha \sim \tau_\alpha^\xi$ with $\xi = 2\lambda/(2 + \lambda)$ which for the present case gives $\xi = 0.4$.

In what follows we compare the CTRW/PEL predictions with the actual MD data in the temperature interval $[0.45, 0.6]$. The lowest temperature is close to the mode-coupling temperature T_c [1]. More specifically we compare three different types of trajectories: (i) continuous trajectory from standard MD simulation, (ii) hopping trajectory between the MB configurations resulting from the same MD simulation, (iii) CTRW trajectory, based on the waiting times which are generated from the above PEL approach.

In a first step we determine the diffusion constant D . By construction (i) and (ii) will result in identical values of D . For the CTRW trajectory one directly obtains $D = a^2/6N \langle \tau \rangle$ where a^2 is a weakly temperature dependent value and can be determined independently [30]. As shown in Fig. 1 the temperature dependent first moment of the waiting time distribution perfectly reflects the T -dependence of $D(T)$. Of course, strictly speaking this comparison is just a consistency check of the CTRW/PEL approach.

In the second step we compare the structural relaxation times τ_α . In the CTRW/PEL approach τ_α is conveniently defined via $\tau_\alpha = \int dt S_0(t)$ where $S_0(t)$ denotes the probability that, starting from a randomly chosen time, the system has not performed a relaxation process [27]. It can be interpreted as the persistence time distribution [31]. Straightforward calculations yields $\tau_\alpha = \langle \tau^2 \rangle / 2 \langle \tau \rangle$ [22, 32]. $S_0(t)$ is shown in Fig. 2 for all considered temperatures. For MD trajectories τ_α is typically extracted from the incoherent scattering function $S(k, t)$. For a comparison of (ii), i.e. the MB hopping trajectory, with (iii) one has to choose a very large value of the wave vector k so that after one discrete hopping process full decorrelation is achieved. Choosing $k = 400$, one can see in Fig. 2 a very good agreement between $S_{MB}(k = 400, t)$ and $S_0(t)$. For $T = 0.6$ it turns out that $S_0(t)$ is slightly more non-exponential. One may speculate that this indicates the onset of anharmonic effects which at temperature $T = 1$ leads to a total breakdown of the PEL approach [33, 34]. For the determination of τ_α we fit S_{MB} with a stretched exponential function $\exp[-(t/\tau_0)_{KWW}^\beta]$. The α -relaxation time τ_α can then be calculated via $\tau_\alpha = \tau_0(k_c)/\beta_{KWW}(k_c)\Gamma(1/\beta_{KWW}(k_c))$.

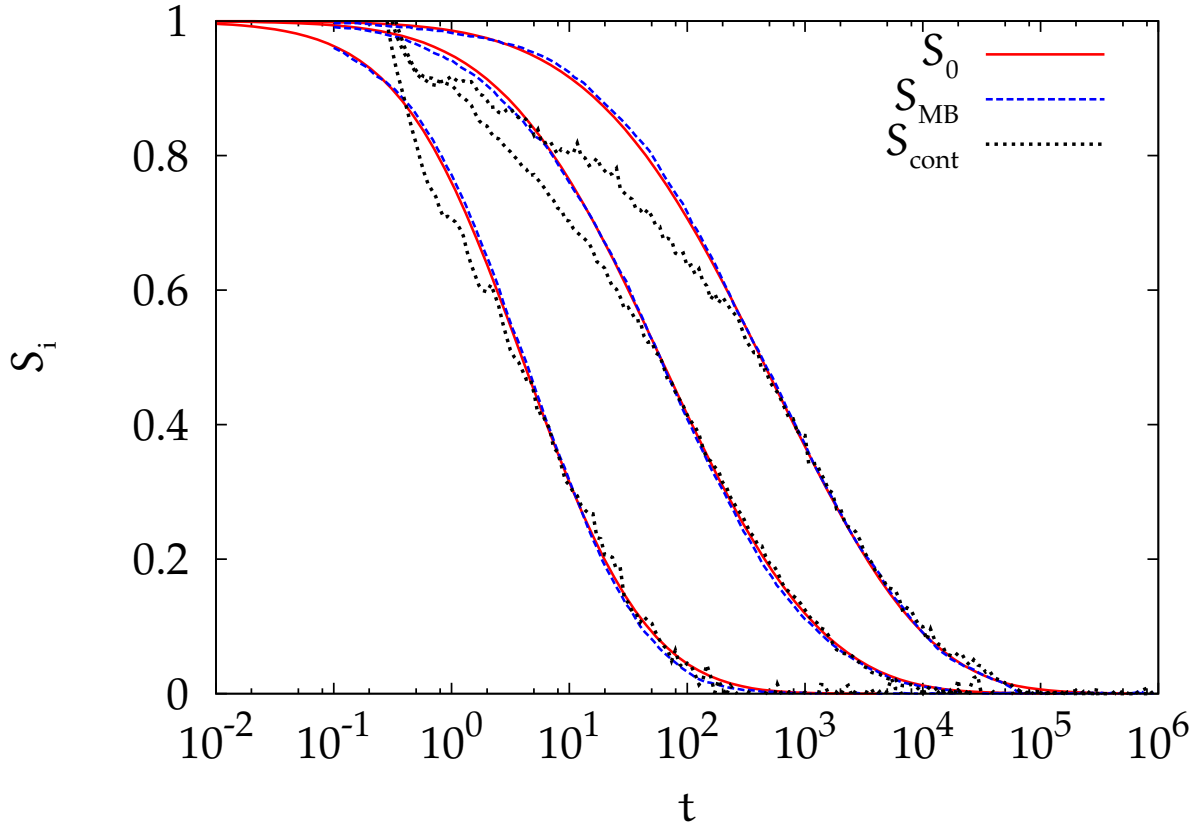


FIG. 2. Comparison of $S_0(t)$ with $S_{MB}(k = 400, t)$ and $S_{cont}(k_c = 15, t)$ for $T = 0.45, 0.5$ and 0.6 .

As expected from the good agreement in Fig. 2 also the τ_α values of (ii) and (iii) agree well as shown in Fig. 1. More subtle is the quantitative comparison with (i) because the additional presence of vibrational and intra-MB processes give rise to additional decorrelation mechanisms for $S_{cont}(k, t)$. These aspects have to be worked carefully because for large system, see Sect. III, we are restricted to use the continuous MD trajectories. We start by fitting $S_{cont}(k, t)$ by a stretched exponential for times in the α -regime, yielding fitting parameters $\tau_0^{cont}(k)$ and $\beta_{KWW}^{cont}(k)$. Their k -dependence for $T = 0.5$ is shown in Fig. 3. The same procedure is performed for the MB trajectory with the corresponding parameters $\tau_0^{MB}(k)$ and $\beta_{KWW}^{MB}(k)$. $\tau_0^{MB}(k)$ and $\tau_0^{coord}(k)$ (calculated from MB respectively real space coordinates) correspond to each other up to a length scale of $k \approx 10$. For larger values of k one finds vibrational dynamics and $\tau_0^{MB}(k)$ saturates, while $\tau_0^{coord}(k)$ further decreases. The plateau values of $\tau_0^{MB}(k)$ and $\beta_{KWW}^{MB}(k)$ we are interested in can now be estimated by finding the value of k_c where $\tau_0^{coord}(k_c)$ and $\beta_{KWW}^{coord}(k_c)$ matches with the MB plateau. We found

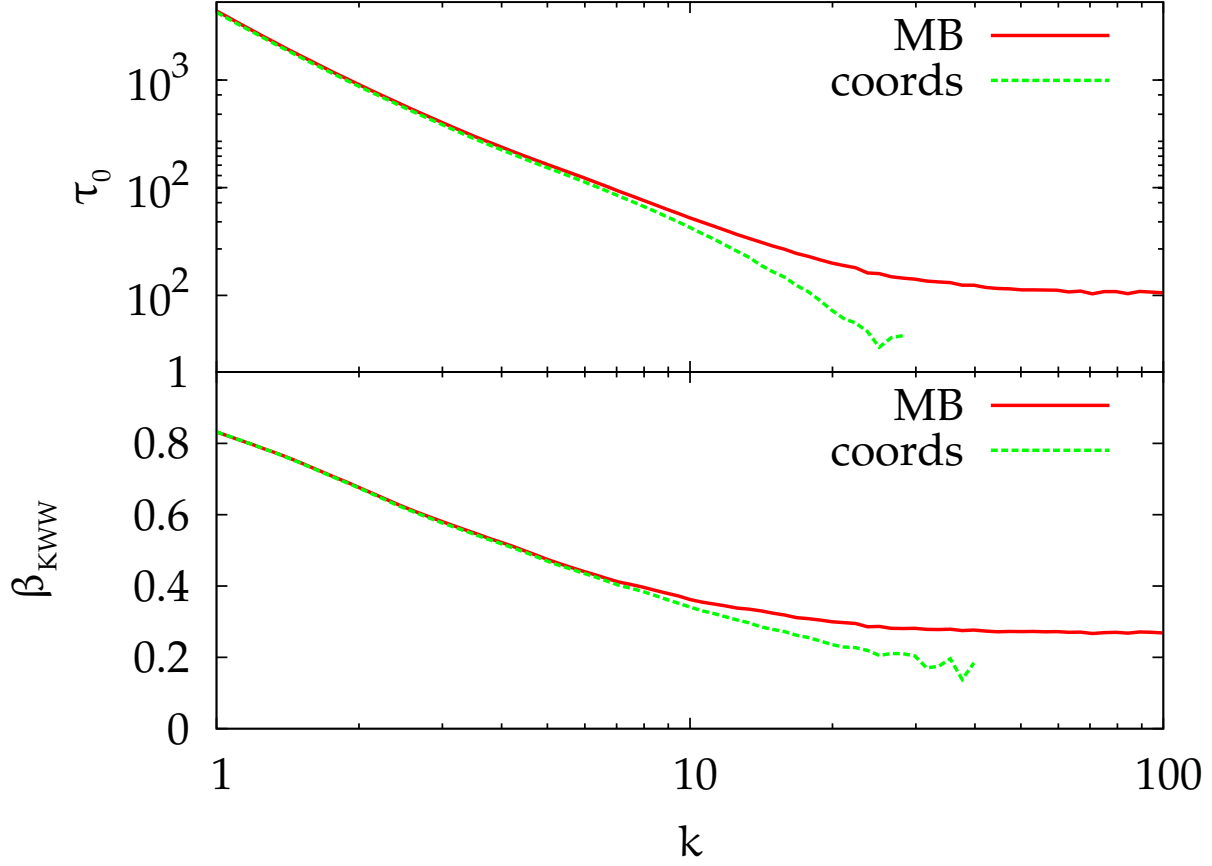


FIG. 3. k dependence of the fit parameter τ_0 and β_{KWW} for the BMLJ65 at $T = 0.5$ for MB and real space coordinates.

$k_c \approx 15$. It is promising and non-trivial that for the same value of k both parameters can be recovered. k_c is slightly temperature dependent, e.g. for $T = 0.6$ one gets $k_c \approx 14 \pm 2$. As shown in Fig. 2 $S_{\text{cont}}(k = k_c, t)$ agrees indeed very well with $S_{MB}(k = 400, t)$. Note that for this comparison the short time decay of $S_{\text{cont}}(k = k_c, t)$ has been scaled out. An equivalent scaling has been already used in Ref. [35] where continuous and IS trajectories had been compared.

III. THE MACROSCOPIC SYSTEM

A. General

With increasing number of particles the properties of MB becomes less useful due to the following reasons: 1) For the minimum system consecutive MB transitions are uncorrelated,

because that during a transition the mobile particles are more or less equally distributed over the sample. In large systems, due to the dynamic heterogeneity, transitions are typically performed by the same mobile particles. Thus, the real space information about the location of a relaxation process is getting important. 2) Due to the many rearranging regions in the sample, the entire system performs a transition in any given fixed time interval, leading to a δ -peaked waiting time distribution. 3) $p_{eq}(e)$ is narrowing when increasing the system size. As a consequence the relation between Γ and e is smeared out and the escape rate is much less correlated with the energy.

As reported in [8], local waiting times remain a precise measure for the dynamics even in large systems. This means that CTRW results can also be applied in large systems. For the comparison with the α -relaxation time τ_α of the large system we have used $S_{\text{cont}}(k_c, t)$ since $S_{MB}(k, t)$ can no longer be defined (see discussion above).

B. Evidence for coupling in a non-equilibrium configuration

So far nothing is known about the size or shape of subsystems, furthermore the kind of coupling is unclear. But how can one identify coupling processes? When studying large systems one faces the problem of strong "dynamic noise" which makes it difficult to distinguish between different coupling events. To minimize the dynamic noise, we prepared a very immobile configuration of a 520 particle system by copying a very stable $N = 65$ structure at $T = 0.5$. From this non-equilibrium structure we calculate the iso-configurational ensemble (IC) to study the distance dependence of possible coupling events between adjacent regions.

At the beginning of each simulation two distinct behaviors can be identified: The a -particles are organized in a stable a -matrix which allows string like motion of b particles without changing the structure significantly. Hence we neglect b particles in the local event calculation. If an a -particle changes its position, it is either a subset of particles exchanging their positions inside the unaltered matrix or it reflects a significant local change of the matrix structure. The first process can be detected via local events but is irrelevant for the decay of the initial structure. The latter gives rise to define *structural* events: When an a -particle performs a local event at time t , we calculate the time averaged coordinates of the tagged particle and the first shell particles at $t \pm \Delta t$ with $\Delta t \approx \tau_\alpha$. To determine if the structure of the first shell changes significantly during the exchange process, we calculate

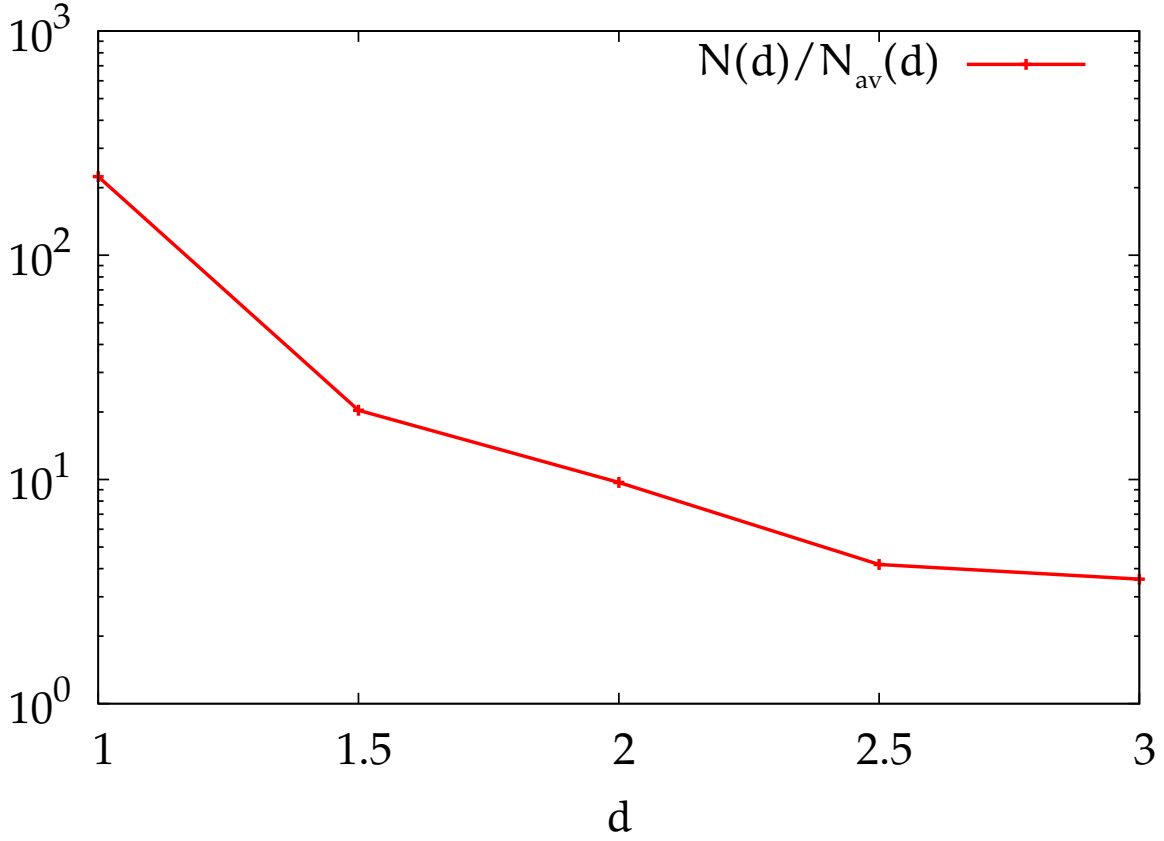


FIG. 4. Number of first events in the distance d normalized by the average number of particles one would expect from the radial distribution function.

the squared displacement $MSD = \sum_i (r_i(t + \Delta t) - r_{i'}(t - \Delta t))^2$ of particle positions before and after the central event. The index i' corresponds to the particle residing closest to the initial position of particle i (allowing permutation). In equilibrium one obtains $\langle MSD \rangle \approx 6$, the distribution is very similar to a Gaussian with a variance close to 2. For the definition of a structural event we use a threshold of 2, above which we call the event structural. The precise choice of the threshold does not change the result.

Before we present the MD results we first discuss possible effects in a small model system: Consider three independent systems with rates $\Gamma_i = \Gamma$. After the first (the left) system changes its state as a consequence of a relaxation process we now discuss the location of the *next* relaxation process. Here we concentrate on the middle and right system. More specifically we discuss the ratio $\langle N_m \rangle / \langle N_r \rangle$ ($\langle N_i \rangle$: the number of next relaxation processes in system i) as well as $\langle \tau_{1,2}^{(m)} \rangle / \langle \tau_{1,2}^{(r)} \rangle$ ($\langle \tau_{1,2}^{(i)} \rangle$ denoting the average waiting time between

the initial process of the left system and the next relaxation process in system i). Since both systems have the same rate one has $\langle N_m \rangle = \langle N_r \rangle = 1$ and $\langle \tau_{1,2}^{m,r} \rangle = 1/2\Gamma$, yielding $\langle \tau_{1,2}^{(m)} \rangle / \langle \tau_{1,2}^{(r)} \rangle = 1$. Now we introduce a coupling mechanism where the initial relaxation enables the central system to acquire the rate $\Gamma_m = 2\Gamma$ whereas the rate Γ_r of right system remains unchanged. Then one naturally has $\langle N_m \rangle / \langle N_r \rangle = 2$ and $\langle \tau_{1,2}^{(m,r)} \rangle = 1/3\Gamma$ for both systems so that again $\langle \tau_{1,2}^{(m)} \rangle / \langle \tau_{1,2}^{(r)} \rangle = 1$. The situation changes if one assumes a distribution of rates $p(\Gamma)$, e.g. $\Gamma_m = 2\Gamma$ and $\Gamma_m = 4\Gamma$ both with probability 0.5. In this case one has $\langle N_m \rangle / \langle N_r \rangle = 3$ and $\langle \tau_{1,2}^{(m)} \rangle / \langle \tau_{1,2}^{(r)} \rangle = 11/12 < 1$. The ratio decreases with increasing width of $p(\Gamma)$.

For the BMLJ system this argument implies that as a consequence of a local coupling mechanism it is by far more likely that the second relaxation process occurs close to the initial one. Averaging over the IC ensemble would observe a significant distance d -dependence $N(d)$. The corresponding distance dependence of $\langle \tau_{1,2} \rangle$ gives information about the strength of the rate fluctuations.

In Fig. 4 we show $N(d)$ normalized by the average number of particles $N_{\text{av}}(d)$ one would expect from the radial distribution function $g(r)$. The curve decays monotonically until a plateau value is reached for $d > 2.5$. As discussed for the model system this is a clear evidence for coupling processes. It would contradict the statistical case where no rate fluctuations are present. The curve roughly reaches a plateau value for $d > 2.5$ giving rise to the assumption that only particles within a sphere of radius $r \approx 2.5$, which is a little bit larger than the minimum system, are directly affected by the first relaxation event. Beyond this sphere, particles hardly recognize the first event, at first, and the changes of the rate become negligible. The discussion of $\langle \tau_{1,2} \rangle (d)$ can be found in Appendix C.

The main contribution of the coupling is therefore between adjacent minimum systems so the coupling range can be restricted to such systems. These results reflect the underlying coupling processes and do not depend on the details of the definition of relaxation events.

C. Physical picture

To illustrate our physical picture of supercooled liquids we make use of the equilibrium distribution of rates $p(\Gamma)$ introduced in [36]. Since thermodynamic properties [19] as well as the diffusivity [8] do not change upon increasing the system size (for $N > N_{\text{min}}$) we strongly

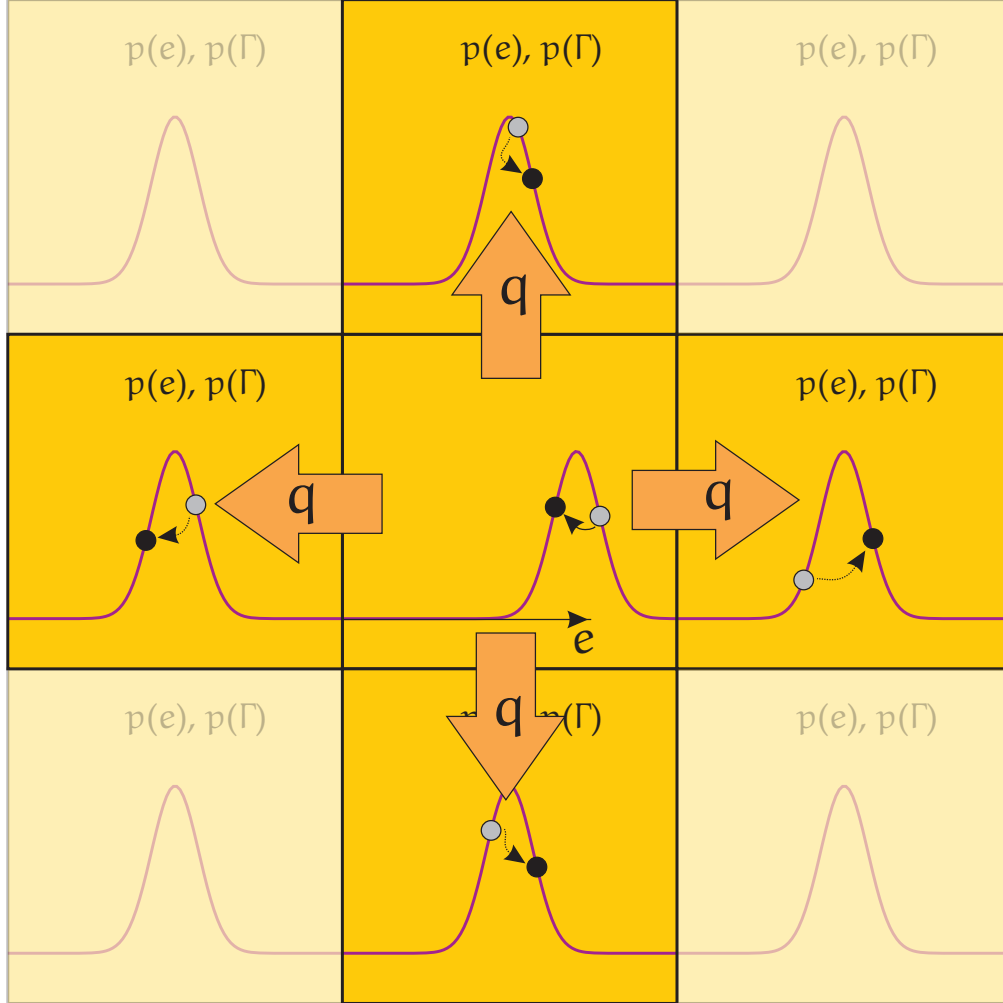


FIG. 5. Schematic sketch of the physical scenario: When the central system relaxes independently (active process, black arrow) the adjacent system may change its mobility without changing its state (passive process, dashed arrow). The role of q is discussed in the text.

suggest that the local equilibrium distribution $p(\Gamma)$ of the mobility does not change either. Therefore we assume that at any arbitrary time a macroscopic system can be decomposed into microscopic subregions of the size of the minimum system which can be described by the properties of their PEL, i.e. by values of e and Γ . When a subregion relaxes, this is called an active process. If one describes a real system by a decomposition into elementary systems, one has to include interactions between these subregions, which is what we call coupling. These interactions allow the subregions to change the rate while keeping their overall Boltzmann distribution $p(\Gamma)$ (passive process), see Fig. 5. Now consider an immobile region adjoining to a rearranging mobile region: The adjacent relaxation enables rate fluctuations

in the slow sample, on average leading to a higher rate. This scenario directly explains the lack of slow regions in large model glass former compared to the minimum system [8]. The fluctuations themselves are interpreted as a coupling mechanism which leads to facilitation like dynamics, sometimes viewed as a hierarchical process [2]. The precise realization of passive processes will be discussed in the next sections. This kind of coarse graining and coupling is in principle captured in the kinetically constrained models, but two important differences remain: 1) All subsystems can always relax independently and 2) a subsystem already contains the complete macroscopic thermodynamics as also realized in the mosaic approach.

D. The coupled landscape Model

Since we have shown that the minimum system can be described by PEL parameters and the CTRW formalism and that localized coupling processes play a major role in supercooled liquids, we bring together both ingredients: We interpret a macroscopic glass former as a set of weakly coupled elementary systems which can be described by their PEL. The elementary systems (ES) are arranged on a square lattice, and their time evolution can be simulated as in [26]. After each active process all coupled adjacent systems are allowed to perform a passive process. We denote this approach as *coupled landscape model* (CLM). It is somehow a minimal model based on the PEL. It has to fulfill the condition that the thermodynamic properties as well as the diffusion coefficient D remain unchanged when increasing the system size.

Dynamic coupling enables so called *passive* processes: Due to active processes of adjacent regions, the mobility (the rate) of an ES can also change without performing a relaxation process. The presence of passive processes must not change the equilibrium distribution $p(e)$. Therefore the transition probability $\pi(e_{old} \rightarrow e_{new})$ to move from state e_{old} to state e_{new} for a passive process has to fulfill

$$\int p(e_{old})\pi(e_{old} \rightarrow e_{new})de_{old} = p(e_{new}) \quad . \quad (5)$$

The latter condition is needed for the probability interpretation. In this paper we focus on the most simple case $\pi(e_{old} \rightarrow e_{new}) = p(e_{new})$, what we call Boltzmann coupling: With the probability q the new rate is simply chosen from the equilibrium distribution. Another

simple case is the Gaussian coupling where e_{new} and e_{old} are correlated, meaning that only small energy changes are allowed. With mean μ and variance σ of the DOS one can define $q(e_{old}, e_{new}) = 1/\sqrt{2\pi s^2} \exp[-(e_{new} - ae_{old} - b)^2/2s^2]$ with constants $a = \sqrt{1 - s^2/\sigma^2}$ and $b = \mu(1 - a)$.

IV. RESULTS

In this section we fix the coupling constant q and show that this model allows a non-trivial reproduction of the most important transport coefficients. This comparison is based on observables, which are well-defined in the MD simulation and the CLM. Here we estimate the coupling strength q based on the α -relaxation time τ_α .

In previous work this kind of dynamical coupling was first estimated within a mean-field approach from the reduction of τ_α when going from $N = 65$ to $N = 130$ particles by a linear expansion in q of the relaxation time $\tau_\alpha(N)$ of the entire system [8]. Here, we follow a more general route which, first, is not based on linear expansion and, second, reflects the transition to macroscopic systems. For the simulations of the CLM we have used a 3^3 system with the parameters listed in table I.

A. α -Relaxation

Again we will use finite size effects of τ_α to estimate q . We increase the system size from N_{\min} to $N = 8320$ and calculate $\tau_\alpha(N)$ from the MD data. $N = 8320$ corresponds to the macroscopic limit for these temperatures. In the CLM one can model this scenario by adding additional ESs. If an ES corresponds to the smallest system in the MD, then one can directly compare the relative reduction of τ_α from an equilibrium simulation. For the dynamical interaction all systems sharing a boundary with the active can experience a passive process.

The MD results show minor finite size effects for D [8]. In several papers this phenomenon is related to hydrodynamic interactions of the sample with its images due to the periodic boundary conditions [37, 38]. However, these hydrodynamic interactions are not captured by the model (D remains constant under coupling). To compare MD and model data, we first have to remove the hydrodynamic effects by scaling D_N and τ_α by D_N/D_{\min} . The

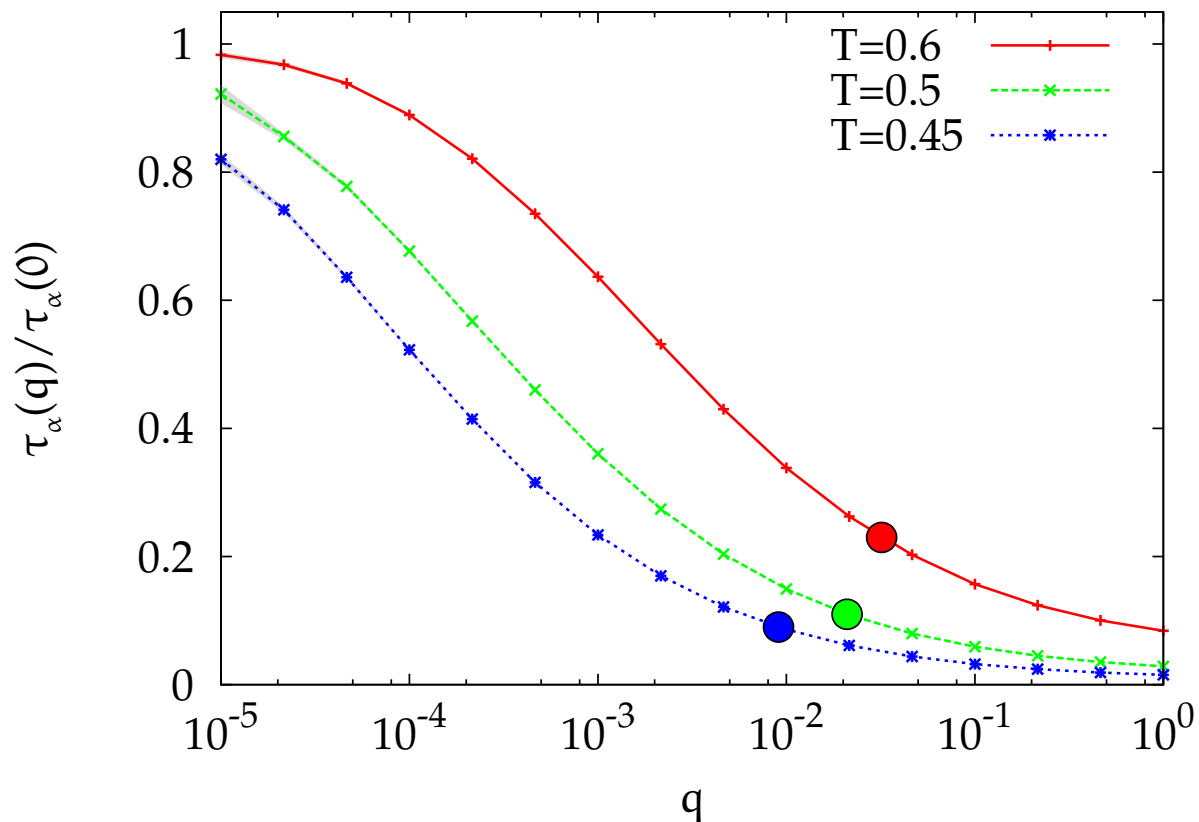


FIG. 6. Relative reduction of τ_α vs. coupling probability q for different temperatures. The solid dots correspond to MD results ($\tau_\alpha(8320)/\tau_\alpha(65) = 0.32, 0.11, 0.08$ for $T = 0.6, 0.5, 0.45$), the gray region corresponds to the error intervals.

correction of τ_α for the largest systems studied is about one order of magnitude smaller than the observed finite size effect itself, so these hydrodynamic effects are negligible for this study.

We determine q by the condition that the reduction of τ_α of the BMLJ system and the CLM exactly match. In Fig. 6 we show the results for three different temperatures. From this analysis we get a temperature dependent coupling constant $q(T)$. In the chosen temperature interval, q decreases by a factor of roughly 3. For small and intermediate values of q_α the empirical formula $\tau_\alpha(q) = \tau_\alpha(0)/(1 + c\sqrt{q})$ fits the data very well. We mention by passing that the reduction does not seem to be analytical in the $q \rightarrow 0$ limit, unlike the linear dependence in q we used earlier in a mean-field approach [8].

The estimation of τ_α provides data for the temperature dependence of q . To answer

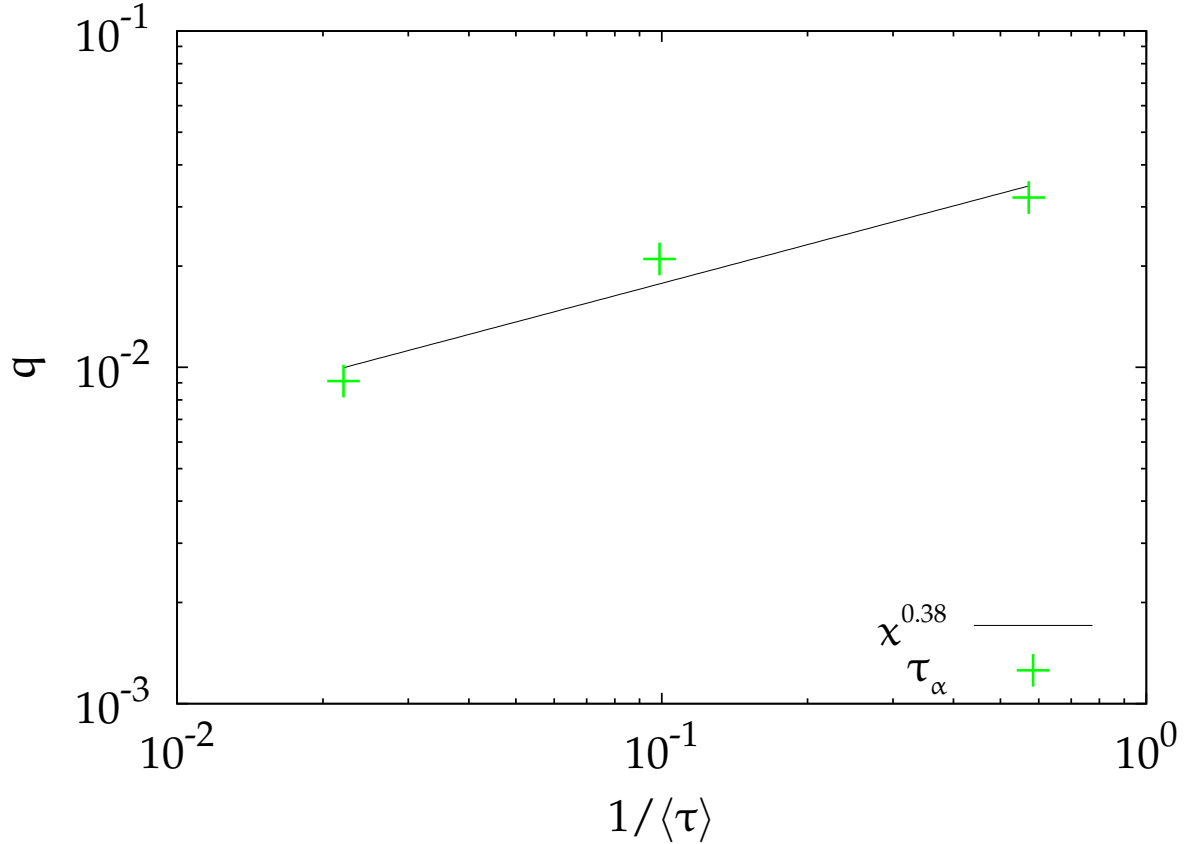


FIG. 7. Coupling constant q vs. average waiting time for different temperatures. The black solid line is a power law as guidance to the eye.

the question how the significance of the facilitation procedure evolves with temperature we compared q with typical timescales in the system. In Fig. 7 a sublinear scaling with $1/\langle\tau\rangle$ can be found, meaning, that with decreasing temperature the number of successful passive processes decreases. At the same time the heterogeneity of the elementary systems increases making a passive process more effective. Both mechanisms compete and we can not determine the total effect on the significance of facilitation. A similar behavior was also found in granular systems [4], where the number of facilitation processes decreases when increasing the density up to the granular glass transition.

Since τ_α depends on the first two moments of φ and the changes of $\langle\tau\rangle$ due to the coupling mechanism are negligible by construction, the reduction of τ_α in Fig. 6 mainly reflects the strong decrease of $\langle\tau^2\rangle$. In Fig. 8 we show the violation of the Stokes-Einstein relation to demonstrate the influence of the coupling processes on the dynamics at different

temperature. The upper black solid line is the analytical result without coupling. The dashed curves correspond to CLM data with constant coupling strength for different values of q and the red line to CLM data with a temperature dependent q with an exponent of $\xi = 0.5$. The decoupling of D and τ_α is obviously strongly reduced by the coupling and ξ does not depend on q in a first order approximation. For low temperatures it reaches the value for large q of approximately 0.175. The prefactor shows a strong q dependence. If one assumes a temperature dependent q , for example $q \sim \langle \Gamma \rangle^{1/2}$, see below for the motivation for this choice, it is also possible to reach intermediate values for ξ . In literature one finds values between $0.05 < \xi < 1/3$, also values around 0.5 are reported for polymers [39–41]).

In Fig. 9 one can see that the CLM results, τ_α and also the non-exponentiality parameter β_{KWW} , match very well with the BMLJ8230 at k_c . At long times the relaxation of the

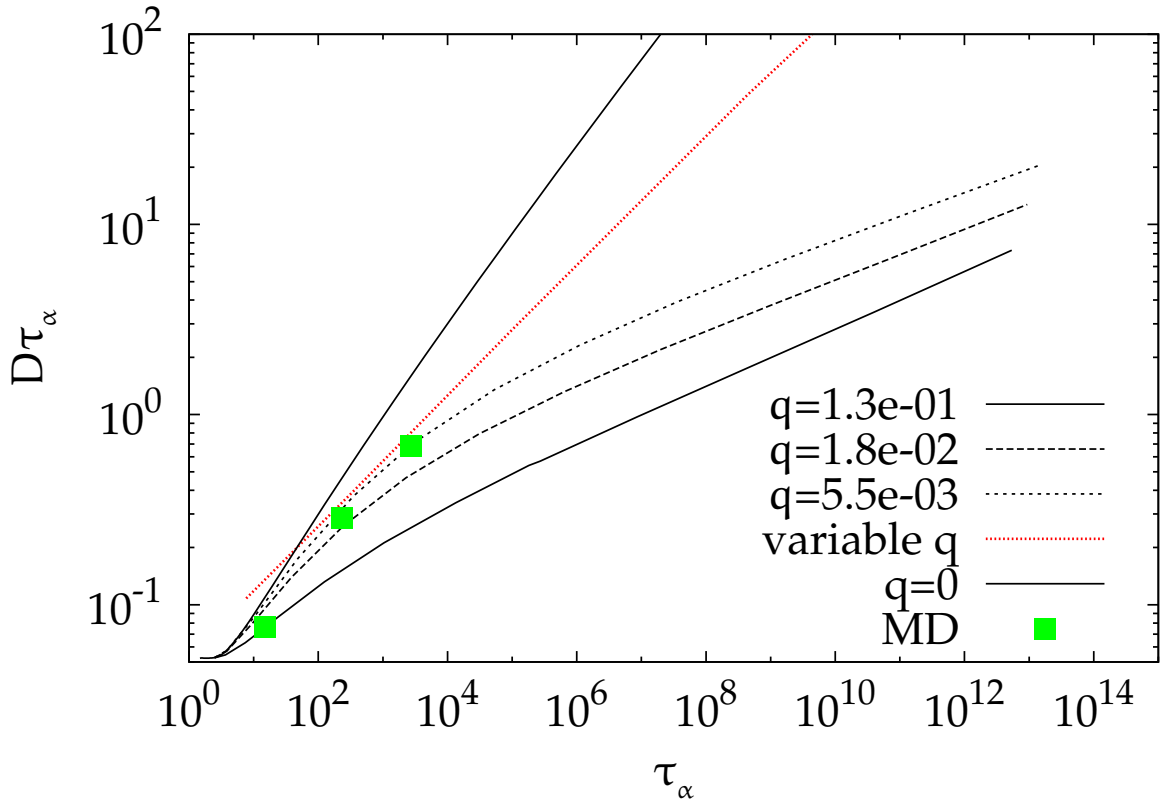


FIG. 8. Effect of the passive processes on the Stokes-Einstein relation: Black lines are calculated with fixed coupling constants, the red one corresponds to a temperature dependent coupling constant, $\propto \langle \Gamma \rangle^{1/2}$, the green points correspond to the MD data.

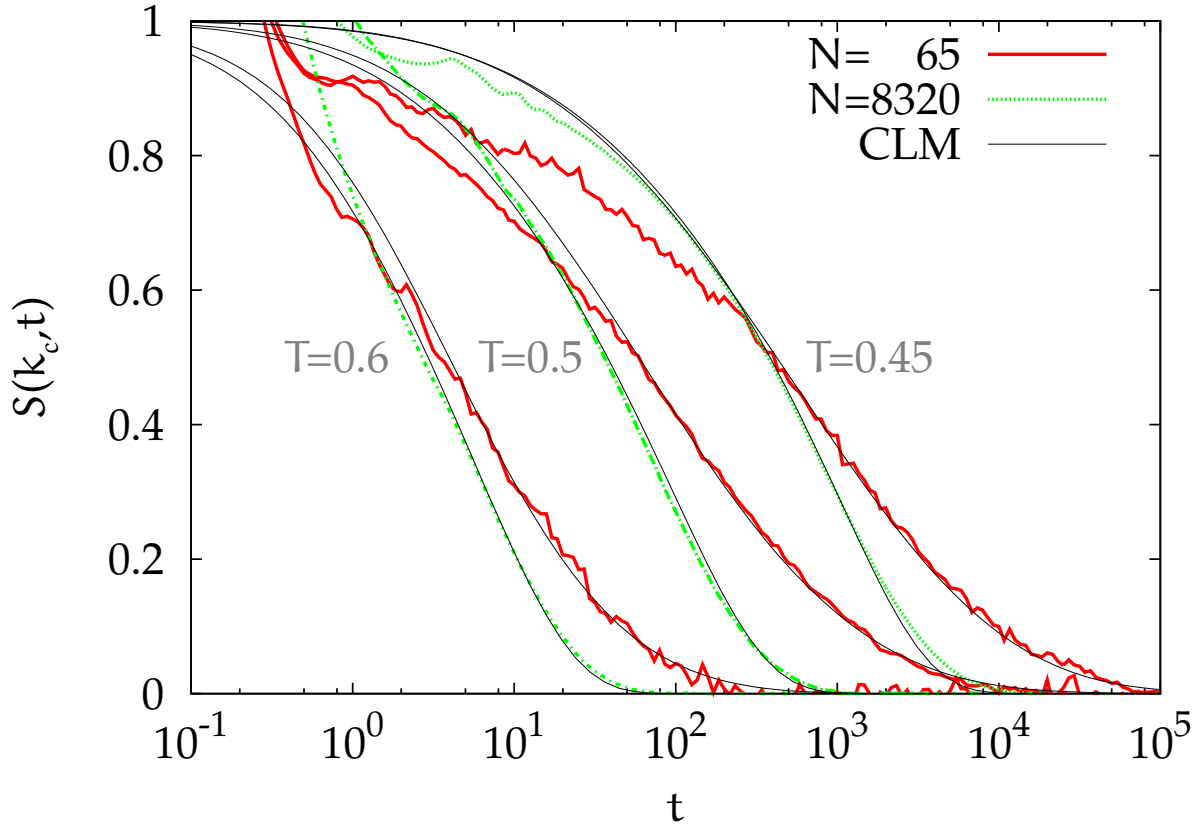


FIG. 9. Overview over $S(k_c, t)$, $S_{\text{cont}}(k_c, t)$ (both scaled for optimal overlap) and $S_0(t)$ from the CLM for $T = 0.6, 0.5, 0.45$ and $N = 65, 8320$.

CLM is a little bit faster than in the MD, at shorter times we find the inverse relation. However, the mismatch is small and can be rationalized by possible heterogeneity of the coupling: For the simulation we have used a fixed coupling constant. One can imagine, that in the microscopic system one has a distribution of coupling constants. The presence of smaller q values immediately leads to slower relaxation at long times, while the presence of larger coupling constants will increase the decay of the relaxation function at short and intermediate times.

B. Discussion

First we want to check how different choices for the geometry of possible passive processes influence our results. Let N_{eff} denote the number of affected systems. In the last section an active process triggers all neighboring ES (sharing a boundary), i.e. $N_{\text{eff}} = 2d$. Other

realizations are possible, e.g. the elastic case: In [9] the authors studied finite size effects of the mechanical loss in thin films of a metallic glass and found that the loss vanishes below a certain thickness of the film. In their view the Eshelby stress field around a plastic zone is up to three times larger than the excitation itself. In dielectric relaxation experiments on glycerol it was found that at low temperatures the relaxation becomes nonlocal and τ_α decreases with system size [11]. The latter effect was not observed in the CLM. However, these effects give rise to some long-range elastic interaction between excitations: An ES can be facilitated with the probability $p(r) \sim r^{-n}$ for $r < r_{\max}$. Hence, every system contributes with r^{-n} to the number of effective interacting systems N_{eff} . This value can be calculated as $N_{\text{eff}} = \sum_i r^{-n}$. As the coupling constant q only describes the probability to perform a passive process for one system, it is useful to introduce the effective coupling strength $q_{\text{eff}} = N_{\text{eff}}q$. Fig. 10 shows τ_α vs. q_{eff} for different interaction lengths r_{\max} and illustrates the importance of q_{eff} as an effective parameter. All curves almost lie on a master curve, so that the distance dependence of the coupling effects only play a very minor role.

One of the most important results is the temperature dependence of q . How can this be interpreted on the level of a single MB transition? One can think of the following physical scenario: Every state has an intrinsic resistance against being facilitated leading to an energy-dependent coupling constant $q(e)$: the lower the energy, the more stable is the MB. This additional factor has, of course, to be considered when choosing the new state to obtain detailed balance. A general e dependence cannot be handled analytically, but for $q(e) = \tilde{q}\Gamma(e)$ one can use the transition probability $\pi \propto \Gamma\varphi$ which generates the correct statistics. If we now calculate q for different temperatures so that $\tau_\alpha(q)/\tau_\alpha(0)$ exactly matches with $\tau_\alpha(\tilde{q})/\tau_\alpha(0)$ we find some temperature dependence for q . Effects along this line may thus rationalize the observed temperature dependence.

C. Conclusion

In a first step we have analyzed in detail how the dynamics of a small BMLJ system with 65 particles can be expressed in terms of PEL parameters. A key step in this endeavor is the fragmentation of the configuration space into MBs, each of which is characterized by an energy. Furthermore, in a simple PEL approach the rate to escape from a given MB is completely characterized by its energy and, more specifically, can be expressed by an effective

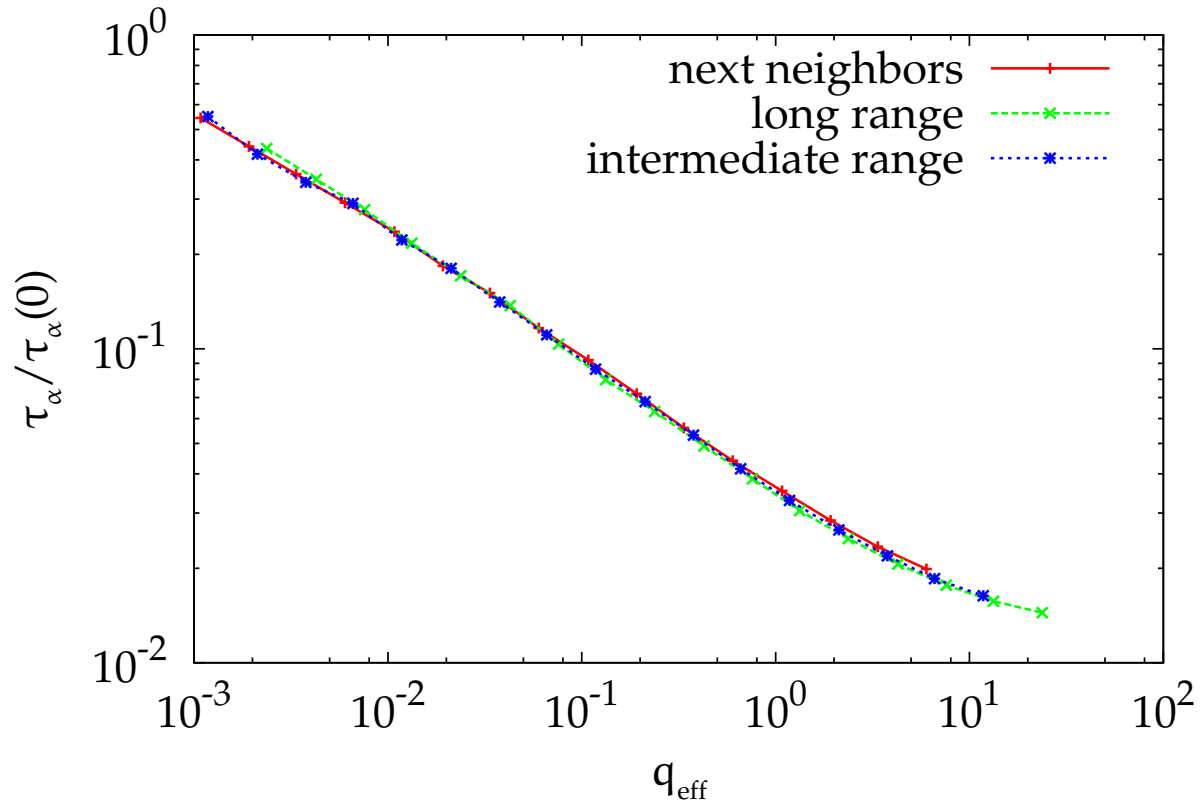


FIG. 10. Relative reduction of τ_α vs. coupling probability q_{eff} for different neighbor geometries. Long range corresponds to $r_{\text{max}} = 5$, intermediate range to $r_{\text{max}} = 2$.

barrier height and an entropic prefactor. Then it is possible to predict the dynamics for all temperatures. For this present case one additional aspect has to be taken into account: a given energy does not fully characterize the escape rate but the escape rate rather follows a relatively narrow distribution as expressed by a log-normal distribution. Intuitively, this reflects the fact that the BMLJ65 system can be interpreted as a superposition of approx. two elementary subsystems [26]. All PEL properties can solely be inferred from an appropriate analysis of the simulation data.

As a consistency check one can estimate, e.g., the diffusivity or the structural relaxation time. Indeed, an excellent agreement is found. Stated differently: the dynamics of the BMLJ65 system is very well understood in terms of the PEL. Of course, due to the discretization the PEL approach cannot resolve properties of the β -relaxation.

In principle one can perform the same MB discretization also for much larger systems.

However, in this case the total energy loses the tremendous information it has for small systems. Because a large system can be decomposed into (roughly) independent smaller systems the same total energy may result from many different realizations. As a consequence many different relaxation rates to escape from this MB are possible. Whereas for small systems the distribution of rates for a given energy is very small as compared to the total distribution of rates (as inferred from the different waiting times) this relation is inverted for large systems. Furthermore, for large system the mapping on the CTRW description is invalidated because of spatial relations.

Therefore one has to complement the PEL approach of small systems by a new concept which takes into account the fact that different regions of the glass-forming system act somehow independently. Our CLM approach is guided by the observation of causal relations between different relaxation processes. Starting from an immobile non-equilibrium system these causal relations can indeed be identified. Via Monte Carlo simulations of the collection of BMLJ65 systems, interacting via the appropriately chosen coupling rules, relevant observables can be determined and compared with the properties of the large BMLJ systems. Interestingly, the precise choice of the coupling rule is not important for the properties of D and τ_α . We carefully identified the wave vector for which the τ_α -value has to be extracted in order to be compatible with the generic structural relaxation time from the CTRW approach. Comparison of the CLM with the actual system allows one to identify a coupling constant q which turns out to be temperature dependent. One may envisage that the resistance of a local region to change its relaxation rate as a consequence of close-by rearrangements becomes larger for lower local energies, then this T -dependence follows quite naturally. Most importantly, the variation of the whole shape of the incoherent scattering function $S_{\text{cont}}(k, t)$ when going from small to large systems can be reproduced by the CLM approach, i.e. by adjusting a single parameter. As a consequence the PEL parameters, defined for the small system, also determine the dynamics of large systems if supplemented by the coupling constant q .

The CLM can be interpreted as a minimum approach to incorporate the dynamic coupling effects which is compatible with the key observation that the thermodynamics as well as the diffusivity only show very small finite size effect. On a qualitative level our model resembles the facilitation approach since immobile regions are typically rendered mobile by the properties of nearby regions and the elementary system size is temperature indepen-

dent. There is, however, one important difference. Whereas in the facilitation approach the elementary systems are just the spins and therefore do not contain any relevant thermodynamic or dynamic information, the elementary building blocks in the present case are small systems which already contain the (nearly) complete information about the thermodynamics and the diffusivity.

In the literature one finds various arguments explaining the observed finite size effect that increasing the system size leads to a decrease of the relaxation time. However, in a comprehensive study Berthier *et al.* showed that this behavior is not universal [42]. If the relaxation time increases with increasing system size this has been related to an activated mechanism (defect diffusion). In contrast, the opposite behavior has been explained in terms of a mode-coupling like mechanisms where the cooperative relaxation occurs via unstable modes. Going to small systems unstable modes may disappear. This explanation is very different to the present PEL approach because here the relaxation mechanism is described by a trapping-type picture rather than by unstable modes.

Karmakar *et al.* found a remarkable correlation of the relaxation time with the configurational entropy [43], supporting the mosaic approach. The data suggest that a system containing approx. 1000 particles can serve as unit system in terms of the configurational entropy which is much larger than the building blocks in the CLM. However, it remains open why already for much smaller systems sizes the diffusivity displays macroscopic behavior. In [44] the authors explain the finite size scaling behavior of τ_α with the existence of a static length scale $\xi(T)$ and an entropic argument: If the system size L is smaller than $\xi(T)$ relaxation processes have to occur on the scale L with a smaller degeneracy factor. In larger systems the degeneracy factor will grow, leading to a lower free energy barrier. In spirit this argument resembles the mode-coupling mechanism from [42]. For the Kob-Andersen system $\xi(T)$ changes by roughly 30% within the chosen temperature interval and our data suggest that a minimum system with around 65 particles is large enough to reproduce the thermodynamics as well as the diffusivity in this temperature interval. Since the minimum system does not show a significant temperature dependence, we can only speculate that the relevant static length scales for all temperatures are already captured by the minimum system.

This entropy-related argument, and the CLM differ in one important point: While the earlier one is based on the free energy barrier height at a *fixed time*, the finite size effect in the

CLM is a consequence of fluctuating barriers (and corresponding jump rates) over a certain *time interval* induced by the facilitation. Since the free barrier from [44] also determines the self diffusion it remains unclear how the different scaling behavior of D and τ_α can be reconciled with this approach. In the CLM, at a fixed time the distribution of rates agrees with the equilibrium distribution of the minimum system. From this distribution directly follows the lack of finite size effects for the thermodynamics and the diffusivity, while the fluctuations effect τ_α exclusively.

It may be interesting to study in future work whether it is also possible to specifically describe the viscosity of large systems via a coupling of small systems. The observed strong correlations between structural relaxation time and viscosity suggest that a similar approach should be possible.

ACKNOWLEDGMENTS

We appreciate the financial support by the DFG (SFB 458 and FOR1394) and we gratefully acknowledge the fruitful discussions and the important input from C. F. Schroer and O. Rubner. We thank L. Berthier for his helpful comments and discussions.

Appendix A: Analytical results

Even in the generalized case it is possible to calculate $\langle \Gamma^n(e) \rangle = \int de p_{eq}(e) \Gamma^n(e)$ analytically as needed for the calculation of D and τ_α . Solving the Gaussian integrals one obtains

$$\ln \left\langle \left(\frac{\Gamma}{\Gamma_0} \right)^n \right\rangle = \frac{n}{2} \lambda \sigma^2 \left[(n\lambda - 2)\beta^2 + k_{\text{entro}}^2 \kappa (n\lambda\kappa - 2) \dots \right. \\ \left. \dots + 2\beta \left(k_{\text{entro}}(\kappa(1 - n\lambda) + 1) + \frac{V}{\lambda\sigma^2} \right) \right], \quad (\text{A1})$$

the transport coefficients then read

$$\ln D \propto \langle \Gamma \rangle = \frac{1}{2} \lambda \sigma^2 (\beta - k_{\text{entro}} \kappa) [\beta(\lambda - 2) - k_{\text{entro}}(\lambda\kappa - 2)] \\ \ln \tau_\alpha \propto \left\langle \frac{1}{\Gamma} \right\rangle = \frac{1}{2} \lambda \sigma^2 (\beta - k_{\text{entro}} \kappa) [\beta(\lambda + 2) - k_{\text{entro}}(\lambda\kappa + 2)] \quad (\text{A2})$$

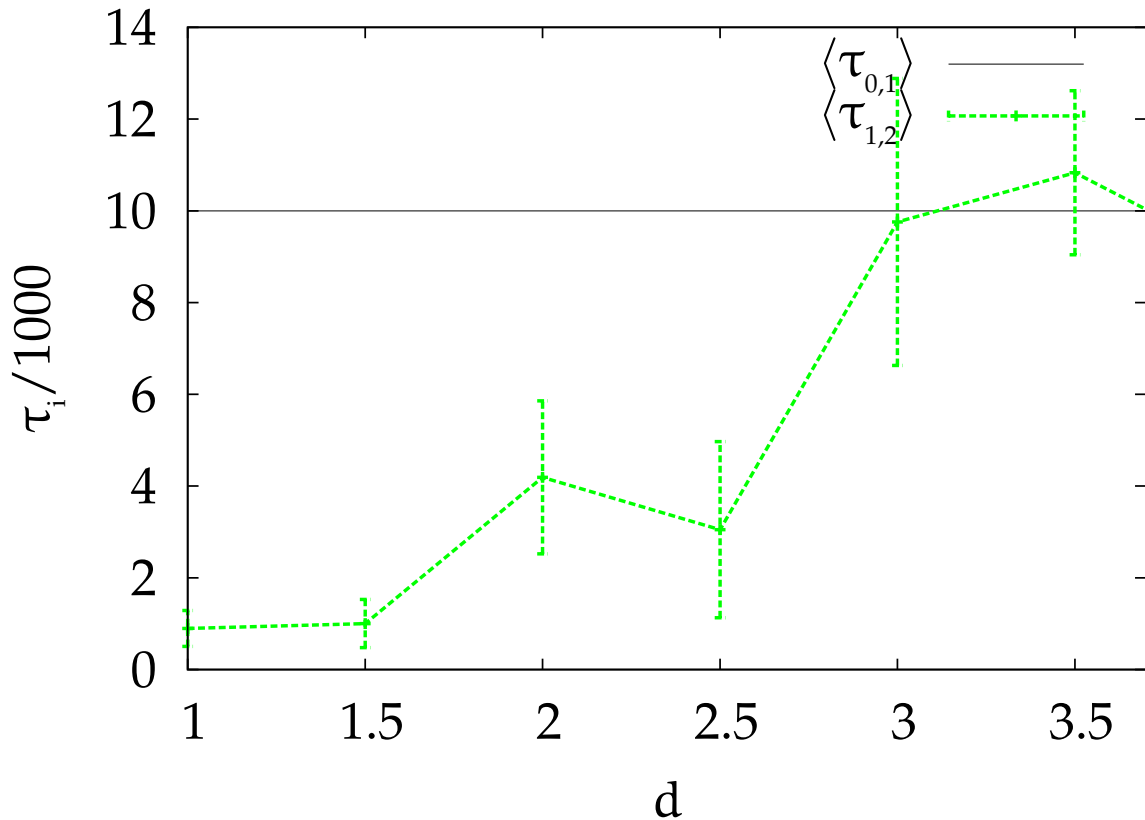


FIG. 11. The different waiting times (for the definition see text) for a MSD threshold of 2 vs. the corresponding distance.

Appendix B: How to handle a system with $\lambda < 1$

When modeling a BMLJ65 with e.g. two independent PEL systems one faces a problem: In the MD one can only access $\Gamma_2(e)$. If one calculates the entire rate $\Gamma_N(e)$ of two PEL systems with $\Gamma_1(e)$ for the model system from [22], the superposition leads to an additional temperature dependent factor $F(T)$ (from the thermodynamic distribution of energies). In the general case it is even possible to end up in an additional energy dependence, making it impossible to extract $\Gamma_1(e)$ from the MD data.

When one uses a single system with $\lambda < 1$ one has to take into account that the persistence time distribution is no longer exponential and has to be determined numerically when simulating the system. Furthermore, $\langle \tau^2(e) \rangle / \langle \tau(e) \rangle^2 > 2$ as obtained in the MD simulation has to be included separately by the distribution $\varpi(\gamma, e)$ (see text). Another result is that the invariance of $\langle \tau \rangle$ under passive processes is no longer valid since $\langle \tau(e) \rangle =$

$1/\langle\Gamma(e)\rangle$ does not hold for $\sigma_\Gamma > 0$. However, this effect is very small and even for high coupling strength smaller than $\approx 4\%$ (at $T = 0.45$).

Appendix C: Waiting times of the non-equilibrium ICE

As discussed in the text a possibility to gain information about the rate fluctuations of the coupling is the waiting time $\langle\tau_{1,2}\rangle(d)$ between the first two structural events in dependence on their distance d . In the case that subsequent relaxation processes are uncorrelated or the coupling mechanism uses a fixed rate one would expect $\langle\tau_{1,2}\rangle(d) = \langle\tau_{0,1}\rangle$. In the presence of coupling with a rate distribution, small d will display small $\langle\tau_{1,2}\rangle(d)$. The results are shown in Fig. 11. We found $\langle\tau_{1,2}\rangle$ increases monotonically with growing distance d up to half of the cell length. Very small values of $\langle\tau_{1,2}\rangle$ are seen for $d < 2.5$, followed by a large jump in $\langle\tau_{1,2}\rangle$. These findings again contradict the statistical case, but since we are in a non-equilibrium configuration we cannot extract information about the strength of the rate fluctuations. The waiting time $\tau_{0,1}$ for the first structural event is also included in the figure. The matching of both observables at large d is to our knowledge highly nontrivial.

-
- [1] M. Vogel, B. Doliwa, A. Heuer, and S. C. Glotzer, *J. Chem. Phys.* **120**, 4404 (2004)
 - [2] A. S. Keys, L. O. Hedges, J. P. Garrahan, S. C. Glotzer, and D. Chandler, *Phys. Rev. X* **1**, 021013 (2011)
 - [3] R. Candelier, A. Widmer-Cooper, J. K. Kummerfeld, O. Dauchot, G. Biroli, P. Harrowell, and D. R. Reichman, *Phys. Rev. Lett.* **105**, 135702 (2010)
 - [4] R. Candelier, O. Dauchot, and G. Biroli, *EPL* **92**, 24003 (2010)
 - [5] G. Adam and J. H. Gibbs, *J. Chem. Phys.* **43**, 139 (1965)
 - [6] J. P. Garrahan and D. Chandler, *Phys. Rev. Lett.* **89**, 035704 (2002)
 - [7] L. O. Hedges, R. L. Jack, J. P. Garrahan, and D. Chandler, *Science* **323**, 1309 (2009)
 - [8] C. Rehwald, N. Gnan, A. Heuer, T. Schröder, J. C. Dyre, and G. Diezemann, *Phys. Rev. E* **82**, 021503 (2010)
 - [9] D. Bedorf and K. Samwer, *J. Non-Cryst. Solids* **356**, 340 (2010)
 - [10] M. Zink, K. Samwer, W. L. Johnson, and S. G. Mayr, *Phys. Rev. B* **73**, 172203 (2006)

- [11] A. A. Pronin, K. Trachenko, M. V. Kondrin, A. G. Lyapin, and V. V. Brazhkin, Phys. Rev. B **84**, 012201 (2011)
- [12] M. Goldstein, J. Chem. Phys. **51**, 3728 (1969)
- [13] R. A. Denny, D. R. Reichman, and J.-P. Bouchaud, Phys. Rev. Lett. **90**, 025503 (2003)
- [14] B. Doliwa and A. Heuer, Phys. Rev. E **67**, 031506 (2003)
- [15] V. K. de Souza and D. J. Wales, J. Chem. Phys. **129**, 164507 (2008)
- [16] J. C. Mauro, R. J. Loucks, and P. K. Gupta, J. Phys. Chem. A **111**, 7957 (2007)
- [17] C. Monthus and J.-P. Bouchaud, J. Phys. A: Math. Gen. **29**, 3847 (1996)
- [18] J. C. Dyre, Phys. Rev. B **51**, 12276 (1995)
- [19] B. Doliwa and A. Heuer, J. Phys.: Condens. Matter **15**, S849 (2003)
- [20] V. Lubchenko and P. G. Wolynes, Annu. Rev. Phys. Chem. **58**, 235 (2007)
- [21] W. Kob and H. C. Andersen, Phys. Rev. E **51**, 4626 (1995)
- [22] A. Heuer, J. Phys.: Condens. Matter **20**, 373101 (2008)
- [23] G. Diezemann and A. Heuer, Phys. Rev. E **83**, 031505 (2011)
- [24] B. Doliwa and A. Heuer, Phys. Rev. Lett. **91**, 235501 (2003)
- [25] S. A. Brawer, J. Chem. Phys. **81**, 954 (1984)
- [26] A. Heuer, B. Doliwa, and A. Saksaengwijit, Phys. Rev. E **72**, 021503 (2005)
- [27] O. Rubner and A. Heuer, Phys. Rev. E **78**, 011504 (2008)
- [28] A. Heuer and A. Saksaengwijit, Phys. Rev. E **77**, 061507 (2008)
- [29] J. P. Garrahan, J. Phys.: Condens. Matter **14**, 1571 (2002)
- [30] B. Doliwa and A. Heuer, Phys. Rev. E **67**, 030501 (2003)
- [31] L. Berthier, G. Biroli, J.-P. Bouchaud, L. Cipelletti, and W. van Saarloos, *Dynamical Heterogeneities in Glasses, Colloids, and Granular Media (International Series of Monographs on Physics)* (Oxford University Press, USA, 2011)
- [32] L. Berthier, D. Chandler, and J. P. Garrahan, EPL **69**, 320 (2005)
- [33] S. Büchner and A. Heuer, Phys. Rev. E **60**, 6507 (1999)
- [34] S. Sastry, P. G. Debenedetti, and F. H. Stillinger, Nature **393**, 554 (1998)
- [35] T. B. Schröder, S. Sastry, J. C. Dyre, and S. C. Glotzer, J. Chem. Phys. **112**, 9834 (2000)
- [36] C. Rehwald, O. Rubner, and A. Heuer, Phys. Rev. Lett. **105**, 117801 (2010)
- [37] D. M. Heyes, J. Phys.: Condens. Matter **19**, 376106 (2007)

- [38] D. M. Heyes, M. J. Cass, J. G. Powles, and W. A. B. Evans, *J. Chem. Phys. B* **111**, 1455 (2007), pMID: 17249725
- [39] F. Mallamace, C. Branca, C. Corsaro, N. Leone, J. Spooren, H. E. Stanley, and S.-H. Chen, *J. Chem. Phys. B* **114**, 1870 (2010), pMID: 20058894
- [40] A. Andraca, P. Goldstein, and L. del Castillo, *Physica A* **387**, 4531 (2008)
- [41] A. Voronel, E. Veliyulin, V. S. Machavariani, A. Kisliuk, and D. Quitmann, *Phys. Rev. Lett.* **80**, 2630 (1998)
- [42] L. Berthier, G. Biroli, D. Coslovich, W. Kob, and C. Toninelli, ArXiv e-prints (2012)
- [43] S. Karmakar, C. Dasgupta, and S. Sastry, *Proc. Natl. Acad. Sci. U. S. A.* **106**, 3675 (2009)
- [44] S. Karmakar and I. Procaccia, ArXiv e-prints (2012)